

EMPIRICAL TEST FOR RELATIVISTIC KINETIC THEORIES BASED ON THE SUNYAEV-ZEL'DOVICH EFFECT

S. M. MOLNAR¹ AND J. GODFREY²

Draft version September 11, 2020

ABSTRACT

We propose a new method to determine the electron velocity (EV) distribution function in the intracluster gas (ICG) in clusters of galaxies based on the frequency dependence of the Sunyaev-Zel'dovich (SZ) effect. It is generally accepted that the relativistic equilibrium EV distribution is the one suggested by Jüttner. However, there is an ongoing debate on the foundation of relativistic kinetic theory, and other distributions have also been proposed. The mildly relativistic intracluster gas (ICG) provides a unique laboratory to test relativistic kinetic theories. We carried out Monte Carlo simulations to generate SZ signal from a single-temperature gas assuming the Jüttner EV distribution assuming a few per cent errors. We fitted SZ models based on non-relativistic Maxwellian, and its two relativistic generalizations, the Jüttner and modified Jüttner distributions. We found that a 1% error in the SZ signal is sufficient to distinguish between these distributions with high significance based on their different best-fit temperatures. However, in any LOS in a cluster, the ICG contains a range of temperatures. Using our N -body/hydrodynamical simulation of a merging galaxy cluster and assuming a 1% error in the SZ measurements in a LOS through a bow shock, we find that it is possible to distinguish between Jüttner and modified Jüttner distributions with high significance. Our results suggest that deriving ICG temperatures from fitting to SZ data assuming different EV distribution functions and comparing them to the temperature in the same cluster obtained using other observations would enable us to distinguish between the different distributions.

Subject headings: galaxies: clusters: general – galaxies: clusters: individual (1E0657–56) – methods: Monte Carlo

1. INTRODUCTION

The generalization of non-relativistic kinetic theory to relativistic velocities is still a subject of debate. Presently, there does not exist a theory of relativistic statistical mechanics that can account for the approach to equilibrium of an ensemble of particles, i.e., a gas, or the relativistic generalization of the many-body problem (for a review see Hakim 2011). The essential difficulty is that, unless all particles in the ensemble originate from the same point in space, they are initially space-like separated. Therefore neither a time-ordering of the particle states, nor their initial conditions can be established. These difficulties impede developing a microscopic theory for how a relativistic gas can achieve thermal equilibrium. Also, treating many-particle interactions within the framework of special relativity in kinetic theories is problematic. Even if we assume that the relativistic gas is in equilibrium, the statistical mechanical treatment of the gas fails because interactions cannot be included in the relativistic Hamiltonian in a consistent manner, since any interaction term in the Hamiltonian would break the Poincaré symmetry (non-interaction theorems, e. g., Leutwyler 1965; Marmo et al. 1984). This is not a problem in nonrelativistic statistical mechanics, because it allows the treatment of interactions between particles based on instantaneous interaction potentials, which are additive in the corresponding Hamiltonian straightforwardly leading to equilibrium velocity distributions.

In 1911, Ferencz Jüttner derived a relativistic generalization of the non-relativistic (Maxwell) velocity distribution, usually referred to as the Jüttner, or Maxwell-Jüttner velocity distri-

bution (Jüttner 1911). For a general introduction to relativistic statistical mechanics, see Sygne (1957). However, problems with the establishment of a self-consistent relativistic kinetic theory led to the question whether the Jüttner distribution is the correct relativistic equilibrium velocity distribution, and other, modified Jüttner distributions were suggested (e.g., Dunkel & Hänggi 2007; Kaniadakis 2006; Lehmann 2006; Schieve 2005; Horwitz et al. 1989). Relativistic molecular dynamics Monte Carlo simulations in one, two, and three dimensions seem to support the Jüttner distribution for equilibrium (Cubero et al. 2007; Montakhab et al. 2009; Peano et al. 2009; Dunkel et al. 2009). These different approaches to relativistic kinetic theory make predictions, in principle testable, and, as we show in this paper, feasible tests are possible. As of today, there is no experimental verification of any of these proposed velocity distributions.

The correct relativistic equilibrium velocity distribution is essential in a variety of applications, including high energy physics, astrophysics, and cosmology (e.g., Dunkel et al. 2007; van Hees et al. 2006; Bernstein 2004; Nozawa et al. 1998; Rephaeli 1995). Therefore, it is of fundamental importance to find experimental or observational methods to derive particle velocity distribution in mildly relativistic gases, which would make it possible to distinguish between the proposed distributions. In this paper we focus on experimental tests of the relativistic Maxwell-Boltzmann distribution as derived by Jüttner (1911), Dunkel & Hänggi (2007) and Horwitz et al. (1981).

The high temperature low density gas of the intracluster gas (ICG) in clusters of galaxies is mildly relativistic, the temperature is not high enough for particle pair creation and annihilation to be important. Thus the ICG provides a unique laboratory to test the proposed velocity distribution functions.

Inverse Compton scatterings of low energy cosmic mi-

¹ Institute of Astronomy and Astrophysics, Academia Sinica, No. 1, Section 4, Roosevelt Road, Taipei 10617, Taiwan, R.O.C.

² Virginia Tech, System Performance Laboratory, 7054 Haycock Road, Falls Church, VA 22043-2311

crowave photons off hot electrons in the ICG, the thermal Sunyaev-Zel'dovich (SZ) effect (Sunyaev & Zeldovich 1980), provides a possibility to study electron velocity (EV) distributions observationally. Calculations of the relativistic SZ effect assume that the EV distribution is in the form of Jüttner distribution (for reviews see, e.g., Birkinshaw 1999; Rephaeli 1995). However, as of today, there is no observational constraints on the EV distribution function in the ICG. Prokhorov et al. (2011) suggested that it may be possible to constrain the EV distribution in the ICG based on the frequency dependence of the SZ effect, and estimated the accuracy needed in the SZ observations. They considered Maxwellian and its relativistic generalization, the Jüttner EV distribution functions. Their method compares the shape of the frequency dependence of the SZ effect based on different EV distribution functions. Prokhorov et al.'s results suggest that, applying their method, SZ measurements with 0.1% accuracy would be necessary to distinguish between Maxwellian and Jüttner velocity distributions.

In this paper we propose a new method to constrain EV distribution functions based on the thermal SZ effect and carry out Monte Carlo simulations to estimate the accuracy necessary to distinguish between the different EV distributions. The structure of this paper is as follows. In Section 2 we give a short discussion about the different approaches to relativistic kinetic theory. We introduce the non-relativistic and relativistic thermal SZ effects in Sections 3 and 4. In Section 4 we also discuss the differences between these approaches and highlight some less known subtleties hidden in their assumptions. We quantify the differences between non-relativistic and relativistic SZ effect at the wide frequency range adopted by the detectors on the *Planck* satellite as well. In Section 5 we fit SZ models to SZ observations of the Bullet cluster based on EV distributions of the form of non-relativistic (Maxwellian), relativistic Jüttner and modified Jüttner. We estimate the accuracy we need in SZ measurements to constrain EV distribution functions with high significance using mock SZ observations in Section 6. We show our results for fits to mock SZ observations of a single-temperature gas in Section 6.1. We fit SZ models to mock observations in a LOS through a bow shock extracted from an N -body/hydrodynamical simulation based on EV distributions of the form of relativistic Jüttner and modified Jüttner in Section 6.2. In Section 7 we discuss our results and the feasibility of our new method to constrain EV distribution functions based on the SZ effect. Section 8 contains our conclusion.

2. DIFFERENT APPROACHES TO RELATIVISTIC KINETIC THEORY

As we mentioned in the Introduction, a relativistic generalization of classical kinetic theory cannot approach equilibrium, yet, we observe in the universe relativistic gas that we believe should be treated as in equilibrium. The difficulties of establishing a self-consistent relativistic kinetic theory can be avoided if we simply assume that a system of relativistic particles, constituting a gas, is in equilibrium, and derive the equilibrium velocity distribution function using macroscopic methods, the principle of maximum entropy, as it was done by Jüttner (Jüttner 1911). The maximum entropy principle (MEP) is particularly apt in this context precisely because we cannot give a microscopic account for how equilibrium is achieved. In a mildly relativistic gas the particle interactions are not so energetic as to significantly involve consideration of pair-creation, there are only two constraints on the entropy: 1) particle number conservation and 2) energy

conservation. Having formed a relativistically invariant Lagrangian, and carefully choosing an invariant measure for the phase space, the Jüttner distribution is obtained (Synge 1957).

The standard classical macroscopic theory assumes the Gibbs entropy functional,

$$S_{NR}[f] = - \int d^3\mathbf{v} f(\mathbf{v}) \log\{f(\mathbf{v})\}, \quad (1)$$

where \mathbf{v} is the 3D velocity. The velocity distribution function is derived by maximizing S_{NR} under the constraints that $f \geq 0$, $\int d^3\mathbf{v} f(\mathbf{v}) = 1$, and the energy conservation, $\langle E \rangle = \int d^3\mathbf{v} f(\mathbf{v}) E(\mathbf{v})$, where the non-relativistic energy, $E(\mathbf{v}) = m\mathbf{v}^2/2$. Note, however, this method works only in Cartesian coordinates, it is not coordinate invariant. Using the relative entropy, the MEP can be cast in a coordinate invariant form (Dunkel et al. 2007). Assuming a reference measure of $\rho(\mathbf{p})$, the relative entropy of $\Phi(\mathbf{p})$ with respect to the reference measure can be written as

$$S[\Phi|\rho] = - \int d^3p \Phi(\mathbf{p}) \log\{\Phi(\mathbf{p})/\rho(\mathbf{p})\}, \quad (2)$$

under the constraints that $\Phi \geq 0$, $\rho \geq 0$, $\int d^3p \Phi(\mathbf{p}) = 1$, and $\langle E \rangle = \int d^3p \Phi(\mathbf{p}) E(\mathbf{p})$, where the relativistic energy, $E(\mathbf{p})^2 = m^2c^4 + \mathbf{p}^2$. Dunkel et al. (2007) showed that adopting a reference measure of $\rho_0 = 1/(mc)^3$, and maximizing the relative entropy, $S[\Phi|\rho_0]$ (Equation 2), one obtains the Jüttner distribution,

$$\Phi_\eta(\mathbf{p}) = \frac{\exp\{-\beta E(\mathbf{p})\}}{Z_\eta E(\mathbf{p})^\eta}, \quad (3)$$

where $\eta = 0$, and Z_η is the partition function. Adopting a reference measure of $\rho_1 = E(\mathbf{p})^{-1}$, the MEP returns the modified Jüttner distribution, Equation 3 with $\eta = 1$. Dunkel et al. (2007) demonstrate that the choice of ρ_0 for the reference measure is associated with translational invariance in the momentum space, while ρ_1 is associated with Lorentz invariance. As we can see, if we require a coordinate invariant form for the MEP, we encounter the questions: Which reference measure should we use? What is the relevant symmetry for the entropy? Since we do not have an established theory for relativistic kinetic theory, the answer is not trivial.

Different approaches to relativistic kinetic theory resulted in particle equilibrium momentum distributions with different values of η in Equation 3. An extension of special relativity was also introduced along the lines suggested by Stueckelberg (Horwitz et al. 1973). The problem of simultaneity is solved by establishing a measure of time common to all particles, on the expense of reinterpretation of relativity. This approach resulted in an equilibrium momentum distribution of the form of Equation 3 with $\eta = 1$ (Horwitz et al. 1981). A different approach was followed by Lehmann (2006). Lehmann noted that the derivation of Jüttner was relativistic, but not covariant. The covariant approach introduced by Lehmann based on Poincaré-invariant constrained Hamiltonian dynamics led to a relativistic one particle momentum distribution function of the form of Equation 3, with $\eta = 2$. Dunkel & Hänggi (2007) were using microscopic collision processes to investigate the relativistic generalization of the Brownian motion. They derived an equilibrium momentum distribution for relativistic particles of the form of the modified Jüttner distribution with $\eta = 1$ (Equation 3).

3. NON-RELATIVISTIC SUNYAEV-ZEL'DOVICH EFFECT

Photons of the cosmic microwave background (CMB), on average, gain energy via inverse Compton scattering off electrons in the ICG in clusters of galaxies, and redistributed to higher frequencies. The intensity change in the CMB due to inverse Compton scattering in clusters assuming non-relativistic (Maxwellian) electron velocity distribution is called non-relativistic SZ effect. Conventionally, the non-relativistic SZ effect is derived using the Kompaneets approximation (Sunyaev & Zeldovich 1980). In the literature, the SZ amplitude derived from the Kompaneets approximation is identified with the non-relativistic thermal SZ effect. However, the Kompaneets approximation is based on more restrictive assumptions, as we will see.

The Kompaneets equation is based on an expansion of the Boltzmann equation, which describes the evolution of the photon occupation number, using a small parameter, $\Delta E_{phot}/(k_B T)$, where E_{phot} is the energy change in the photons due to inverse Compton scattering, T is the electron temperature, and k_B is the Boltzmann constant (Kompaneets 1957). The Kompaneets approximation assumes that the isotropic incoming photons have a thermal (Planckian) spectrum, the isotropic electron velocity distribution is Maxwellian, and the energy change in the photons, ΔE_{phot} is small, $\Delta E_{phot}/(k_B T) \ll 1$. This method is using the Thompson scattering cross section in the rest frame of the CMB instead of the rest frame of the electron assuming that the electron velocities are small, thus the Lorentz transformations between the two rest frames can be ignored.

Sunyaev and Zel'dovich assumed that the photon occupation number, n , and x_e are small in the ICG, thus terms proportional to n and n^2 can be ignored relative to $\partial n/\partial x_e$. In this case the Kompaneets equation simplifies to

$$\frac{\partial n}{\partial y} = \frac{1}{x_e^2} \frac{\partial}{\partial x_e} \left[x_e^4 \left(\frac{\partial n}{\partial x_e} \right) \right], \quad (4)$$

where the dimensionless frequency is $x_e = h_P \nu / (k_B T)$, and h_P is the Planck constant, the Compton- y parameter is $y = \int \Theta d\tau$, where the dimensionless electron temperature is $\Theta = (k_B T)/(m_e c^2)$, m_e is the mass of the electron, and the optical depth, τ is defined as $d\tau = \sigma_T n_e dl$, where σ_T is Thomson scattering cross-section, n_e is the electron number density, and dl is the line element along the LOS.

Changing the dimensionless frequency x_e to $x_\nu = h_P \nu / (k_B T_{CMB})$, where T_{CMB} is the temperature of the CMB, does not change the right hand side of Equation 4, and changing variables from $n(x_\nu, y)$, to $n(\ln x_\nu + 3y, y)$, Equation 4 can be transformed into a form of diffusion equation. This diffusion equation can be solved analytically, and since the intensity is proportional to $x^3 n$, the intensity change can be expressed as

$$\Delta I_K(x_\nu, T) = y \frac{i_0 x_\nu^4 e^{x_\nu}}{(e^{x_\nu} - 1)^2} \left(x_\nu \frac{e^{x_\nu} + 1}{e^{x_\nu} - 1} - 4 \right), \quad (5)$$

where the Compton- y parameter is $y = \int \Theta d\tau$, where the optical depth, τ is defined as $d\tau = \sigma_T n_e dl$, where σ_T is Thomson scattering cross-section, n_e is the electron number density, and dl is the line element along the LOS, and the conversion factor, i_0 , is

$$i_0 = 2(k_B T_{CMB})^3 / (h_P c)^2. \quad (6)$$

In this approximation, at constant temperature in the line of sight (LOS), $\Delta I_K \sim \tau$, which shows that it is essentially a sin-

gle scattering approximation (also verified with Monte Carlo simulations; Molnar & Birkinshaw 1999). In the single scattering approximation the photon and electron distributions are isotropic, in accordance with the original assumptions. Note, that single scattering, in most cases, is an adequate approximation in the ICG, since the optical depth integrated along a LOS through a cluster is $\tau = \int \sigma_T n_e dl \lesssim 0.01$.

In the Kompaneets approximation, only the amplitude of the SZ effect depends on the electron temperature, the shape of the effect as a function of frequency is the same. As a consequence, the crossover frequency, $\nu_0 = 217.7$ GHz, where the SZ amplitude is zero ($\Delta I_K[\nu_0] = 0$) and the amplitude changes from decrement in the CMB to increment, is independent of the electron temperature.

4. RELATIVISTIC SUNYAEV-ZEL'DOVICH EFFECT

The Kompaneets approximation has been and is widely used to calculate the SZ signal, since it can be easily calculated, as it provides an analytic expression (for reviews see Carlstrom et al. 2002; Birkinshaw 1999). However, it was realized that, at the high-temperature ICG (~ 15 keV), the gas is mildly relativistic, thus a relativistic generalization of the non-relativistic Maxwellian velocity distribution should be used at mm/submm wavelengths (Rephaeli 1995).

The relativistic treatment of the inverse Compton scattering in mildly relativistic electrons (applicable in the ICG) without assuming that the photon energy change is small was derived by Wright (1979). Wright's method adopts the Thompson scattering cross section in the rest frame of the electron instead of the rest frame of the CMB, and uses Lorentz transformations between them.

Following Wright, we express the frequency change due to inverse Compton scattering between an electron with velocity $\beta = v/c$ (where c is the speed of light) as a function of the logarithm of the ratio of the frequencies of the scattered and input photons, ν and ν_0 , in the Lab frame,

$$s = \ln \left[\frac{\nu}{\nu_0} \right] = \ln \left[\frac{1 + \beta \mu_2}{1 - \beta \mu_1} \right], \quad (7)$$

where we also expressed the ratio of the frequencies in the rest frame of the electron, where the photon scattered from an input cosine angle $\mu_1 = \cos \varphi_1$ to $\mu_2 = \cos \varphi_2$ relative to the z axis (z is parallel to the velocity of the electron).

We use the Wright's formalism in the single scattering limit, which is appropriate in the ICG with low optical depth. In this approximation, the probability that a single photon scattering with an electron with a velocity of β (in units of c) results in a frequency shift described by s , the frequency redistribution function, $P_1(s, \beta)$, can be expressed in the electrons's rest frame, as

$$P_1(s, \beta) ds = \int p_\mu(\mu_1) \phi(\mu_2 | \mu_1) d\mu_1 \frac{d\mu_2}{ds}, \quad (8)$$

where $p_\mu(\mu_1)$ is the probability that the electron scatters with a photon having an incoming cosine angle μ_1 , and $\phi(\mu_2 | \mu_1)$ is the conditional probability of photons scattering into cosine angle μ_2 if the initial photon direction cosine was μ_1 ($\mu_1 \rightarrow \mu_2$) in the rest frame of the electron (Chandrasekhar 1960):

$$\phi(\mu_2 | \mu_1) d\mu_2 = \frac{3}{8} \left[1 + \mu_1^2 \mu_2^2 + \frac{1}{2} (1 - \mu_1^2)(1 - \mu_2^2) \right] d\mu_2. \quad (9)$$

$p_\mu(\mu_1)$ can be derived from transforming an isotropic incoming photon direction distribution to the rest frame of the electron,

$$p_\mu(\mu_1)d\mu_1 = [2\gamma^4(1-\beta\mu_1)^3]^{-1}d\mu_1, \quad (10)$$

where $\gamma^2 = 1/(1-\beta^2)$. The frequency redistribution function due to Compton scattering, the probability for a single scattering resulting a frequency shift s in the Lab frame, thus can be expressed as

$$P_1(s, \beta)ds = \frac{1}{2\gamma^4\beta} \int_{\mu_a}^{\mu_b} d\mu_1 \frac{1+\beta\mu_2}{[1-\beta\mu_1]^3} \phi(\mu_2|\mu_1)ds, \quad (11)$$

where the limits of the integral, μ_a and μ_b are determined by the condition that the cosines have to be real:

$$\mu_a = \begin{cases} -1 & s \leq 0 \\ [1 - e^{-s}(1+\beta)]/\beta & s \geq 0 \end{cases} \\ \mu_b = \begin{cases} [1 - e^{-s}(1-\beta)]/\beta & s \leq 0 \\ 1 & s \geq 0. \end{cases} \quad (12)$$

The integral over μ_1 can be performed analytically (e.g., [Molnar 2015](#)).

The frequency redistribution function, P_1 , as a function of s , can be obtained by integrating over the velocity distribution of the electrons, $p_e(\beta)d\beta$, assuming that it is known,

$$P_1(s) = \int_{\beta_0}^1 P_1(s, \beta)p_e(\beta)d\beta, \quad (13)$$

where the lower limit β_0 is the minimum electron velocity needed to get frequency shift s ,

$$\beta_0 = \frac{e^{|s|}-1}{e^{|s|}+1}. \quad (14)$$

Note that carrying the integral over μ_1 analytically, our integral in Equation 13 is only one dimensional. In general, this integral needs to be performed numerically.

The intensity at frequency ν , after single scatterings, $I_1(\nu)$, can be expressed as a convolution of the incoming intensity, $I_0(\nu_0)$, assumed to be isotropic, and the single scattering probability distribution, $P_1(s)$,

$$I_1(\nu) = \int_{-\infty}^{\infty} ds P_1(s)I_0(\nu_0), \quad (15)$$

where the integral is over $s = \ln(\nu/\nu_0)$ with the frequency after scattering, ν , fixed, and $P_1(s)$ is given by Equation 13.

In the single-scattering approximation, the probability that a photon passes the ICG without scattering is $e^{-\tau}$, and the chance that is scattered once is $\tau e^{-\tau}$. Thus the full frequency redistribution function, which describes the frequency change after the photons pass through the ICG, becomes

$$F_1(s) = (1-\tau)\delta(s) + \tau P_1(s), \quad (16)$$

and the emergent intensity can be expressed as a convolution,

$$I_{SZ}(\nu) = \int_{-\infty}^{\infty} ds F_1(s)I_0(\nu_0). \quad (17)$$

Thus, assuming that the incoming photon frequency distribution is Planckian in the Lab frame, the change in the emerging intensity, $I_{SZ}(\nu) - I_0(\nu)$, the thermal SZ effect, becomes

$$\Delta I_{SZ}(\nu) = i_0\tau \int ds P_1(s) \left(\frac{x_0^3}{e^{x_0}-1} - \frac{x_\nu^3}{e^{x_\nu}-1} \right), \quad (18)$$

where $x_0 = h_P\nu_0/(k_B T_{CMB})$, and i_0 is defined as in Equation 6.

Assuming that the electron equilibrium velocity distribution function is non-relativistic (Maxwellian),

$$p_{MX}(\beta)d\beta = N_{MX}\beta^2 \exp\{-\beta^2/(2\Theta)\}d\beta, \quad (19)$$

where N_{MX} is the normalization, we obtain a non-relativistic approximation of the SZ effect, ΔI_{NR} from Equation 18. However, contrary to the conventional non-relativistic SZ effect based on the Kompaneets approximation, this method uses the Wright formalism, and does not ignore the Lorentz transformations between the rest frame of the electron and the CMB.

[Wright \(1979\)](#) calculated the SZ amplitude using the relativistic generalization of the Maxwellian velocity distribution derived by [Jüttner](#),

$$p_J(\beta)d\beta = N_J \frac{\gamma^5 \beta^2}{\Theta} \exp\{-\gamma/\Theta\}d\beta, \quad (20)$$

where N_J is the normalization for the probability distribution. The relativistic SZ effect based on the Jüttner velocity distribution, ΔI_J , can be derived using Equation 20 in Equation 18.

We use the modified Jüttner distribution in the form of

$$p_{MJ\eta}(\beta)d\beta = N_{MJ\eta} \frac{\gamma^5 \beta^2}{\gamma^\eta \Theta} \exp\{-\gamma/\Theta\}d\beta, \quad (21)$$

where $N_{MJ\eta}$ is the normalization for the modified Jüttner electron velocity distribution ([Lehmann 2006](#); [Dunkel & Hägggi 2007](#)). The modified Jüttner distribution differs from the Jüttner distribution only in the power of γ , $p_{MJ\eta} \sim p_J/\gamma^\eta$ (e.g., [Dunkel et al. 2007](#)). We derive the relativistic SZ effect based on the modified Jüttner velocity distribution, $\Delta I_{MJ\eta}$, using Equation 18.

As an illustration, in Figure 1, we show the intensity change in the CMB due to the Sunyaev-Zel'dovich effect (in units of $i_0\tau$, where τ is the optical depth and i_0 is given by Equation 6) as a function of frequency (in GHz) for electron temperatures of 15.33 keV and 5.11 keV (upper and lower set of lines). Solid, dashed, and dotted lines represent SZ amplitudes assuming electron velocity distribution functions of the form of relativistic Jüttner (Equation 20), modified Jüttner with $\eta = 1$ (Equation 21), and non-relativistic, Maxwellian (Equation 19) using the Wright formalism (ΔI_J , ΔI_{MJ1} , and ΔI_{MX}). Dash-dotted lines show the non-relativistic SZ amplitude derived based on the Kompaneets approximation (ΔI_K). The squares, triangles, and plus signs represent SZ amplitudes assuming relativistic Jüttner and Maxwellian velocity distributions based on the Wright formalism, and amplitudes using the Kompaneets approximation at the frequencies of the *Planck* instruments ($\nu = 30, 44, 70, 100, 143, 217, 353, 545$, and 857 GHz; e.g., [Bourdin et al. 2017](#); note, the *Herschel-SPIRE* instrument also covers the 600 and 857 GHz frequency channels with higher spatial resolution; [Griffin et al. 2010](#)).

Figure 1 demonstrates that the differences between SZ amplitudes derived from the Kompaneets approximation (dash-dotted lines) and those derived from the Wright formalism

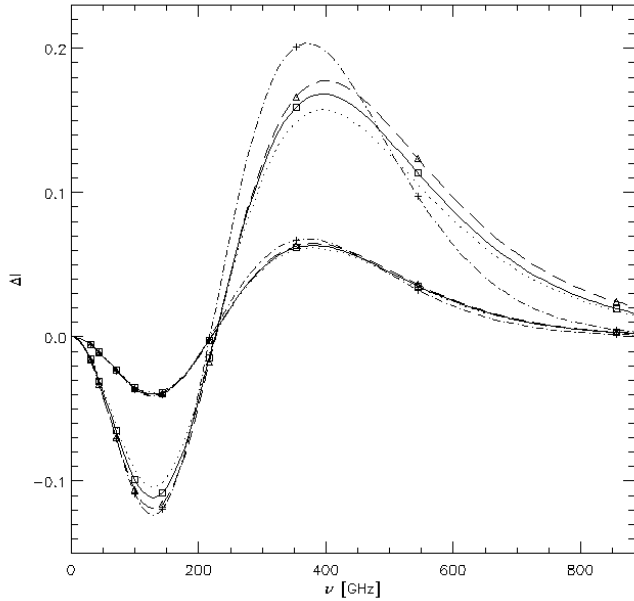


FIG. 1.— The Sunyaev-Zel'dovich effect (in units of $i_0\tau$) as a function of frequency (in GHz) for electron temperatures of 15.33 keV and 5.11 keV (upper and lower set of lines). Solid, dotted, and dashed lines represent SZ amplitudes assuming electron velocity distribution functions of the form of relativistic Jüttner, modified Jüttner with $\eta = 1$, and non-relativistic Maxwellian using the Wright formalism. Dash-dotted lines show the non-relativistic SZ amplitude derived using the Kompaneets approximation. The squares, triangles, and plus signs represent the corresponding SZ amplitudes at the frequencies of the *Planck* instruments.

using Maxwellian velocity distribution (dashed lines) relative to those derived from assuming Jüttner distribution (solid lines) are larger (e.g., ΔI_K is much larger than ΔI_J or ΔI_{MX} at 350 GHz). As a consequence, we obtain a better non-relativistic approximation for the SZ effect using the Wright method assuming a Maxwellian velocity distribution as opposed to using the Kompaneets equation. Thus, the main difference between the amplitudes of the SZ effect based on the Kompaneets approximation and the relativistic SZ effect using the Wright method is not the form of the velocity distribution used (Maxwellian vs. Jüttner), but the treatment of the collision process (compare dashed and dash-dotted lines to the solid lines in Figure 1). The kompaneets approximation over(under) estimates the SZ signal at frequencies $\lesssim 450$ GHz ($\gtrsim 450$ GHz). In Table 1 we quantify these differences. In this table we show the ratios between SZ amplitudes derived from the Kompaneets approximation over those based on the Wright formalism assuming Jüttner distribution, $\Delta I_K/\Delta I_J$, and Maxwellian distribution, $\Delta I_K/\Delta I_{MX}$, at electron temperatures of $T = 15.55$ keV and $T = 5.11$ keV.

At high electron temperatures, e.g., $T = 15$ keV, the error due to using the Kompaneets approximation instead of the Wright formalism with the Jüttner (or Maxwellian) distribution is $\gtrsim 10\%$ for $\nu \gtrsim 100$ GHz (or $\nu \gtrsim 217$ GHz). At the highest *Planck* frequency, $\nu = 857$ GHz, ΔI_K and ΔI_{MX} are lower than ΔI_J by a factor of 4 and 5 ($\Delta I_K/\Delta I_J = 0.25$, $\Delta I_K/\Delta I_{MX} = 0.2$). Even at lower temperatures, ΔI_K deviates from ΔI_J by $\gtrsim 8\%$, and at $\nu = 857$ GHz ΔI_K is a factor of 2 too small ($\Delta I_K/\Delta I_J \sim \Delta I_K/\Delta I_{MX} \sim 0.5$). Thus, Table 1 demonstrates that at high *Planck* frequencies ($\nu \gtrsim 217$ GHz), even for lower ICG temperatures ($T \sim 5$ keV), the Wright formalism should be used to calculate the SZ signal either with the Jüttner, or Maxwellian velocity distribution instead of the

TABLE 1
SZ AMPLITUDE RATIOS AT *Planck* FREQUENCIES USING DIFFERENT METHODS FOR $T = 15.55$ keV AND 5.11 keV.

| Freq. GHz | $\Delta I_K/\Delta I_J$ ^a | $\Delta I_K/\Delta I_{MX}$ ^b | $\Delta I_K/\Delta I_J$ ^c | $\Delta I_K/\Delta I_{MX}$ ^d |
|--------------|--------------------------------------|---|--------------------------------------|---|
| | $T = 15.5$ keV | $T = 15.5$ keV | $T = 5.1$ keV | $T = 5.1$ keV |
| 30 | 1.06 | 0.98 | 1.02 | 0.99 |
| 44 | 1.06 | 0.99 | 1.02 | 1.00 |
| 70 | 1.08 | 1.01 | 1.03 | 1.00 |
| 100 | 1.10 | 0.93 | 1.03 | 1.01 |
| 143 | 1.11 | 1.03 | 1.04 | 1.01 |
| 217 | 0.11 | 0.09 | 0.24 | 0.22 |
| 353 | 1.26 | 1.20 | 1.08 | 1.06 |
| 545 | 0.86 | 0.79 | 0.92 | 0.89 |
| 857 | 0.25 | 0.20 | 0.53 | 0.50 |

^a SZ amplitudes derived from the Kompaneets approximation over those based on the Wright formalism assuming Jüttner velocity distribution at $T = 15.55$ keV.

^b SZ amplitudes derived from the Kompaneets approximation over those based on the Wright formalism assuming Maxwellian velocity distribution at $T = 15.55$ keV.

^c Same as *a* but for $T = 5.11$ keV.

^d Same as *b* but for $T = 5.11$ keV.

Kompaneets approximation. However, the Kompaneets approximation is still widely used at all *Planck* frequencies (e.g., Baldi et al. 2019; Planck Collaboration et al. 2016).

In contrast to the non-relativistic SZ effect (based on the Kompaneets approximation), the shape of the relativistic SZ effect (derived using the Wright formalism) as a function of frequency does depend on the temperature as well. This makes it possible to use the frequency dependence of the SZ effect to derive the temperature of the ICG (e.g., Pointecouteau et al. 1998; Hansen et al. 2002). Other methods also have been proposed to derive the temperature in the ICG using the frequency dependence of the relativistic SZ effect based on the shift of the crossover frequency from $\nu_0 = 217.7$ GHz (Rephaeli 1995), the slope of the SZ effect near the crossover frequency (Colafrancesco et al. 2009), and the ratio of the SZ intensities at two different frequencies (Prokhorov et al. 2010).

5. FITTING TO SZ OBSERVATIONS OF THE BULLET CLUSTER

The Bullet cluster (1E0657–56) is one of the few high-infall velocity merging galaxy clusters, which provided the first direct evidence for the existence of dark matter based on multi-frequency observations (Clowe et al. 2006). The offset between the mass surface density centers derived from gravitational lensing and the X-ray emission peaks marking the gas (baryonic) component were significant (200–300 kpc, e.g., Paraficz et al. 2016).

We illustrate our proposed method to determine the EV distribution function in the ICG in clusters of galaxies based on the frequency dependence of the SZ effect using SZ observations of the Bullet cluster. We use archival SZ observations of the Bullet cluster available at four frequencies: 150, 275, 600, and 857 GHz (Gomez et al. 2004; Halverson et al. 2009; Plagge et al. 2010; Zemcov et al. 2010). We show the SZ observations as a function of frequency in Figure 2 (squares with error bars). We assume that the optical depth is unknown, and treat it as a nuisance parameter, therefore our method is sensitive only to the shape of the SZ signal. Note, that if the optical depth were known with high precision, the SZ amplitudes could also be used and it would be easier to distinguish between different velocity distributions (see Figure 1). We adopt a χ^2 statistic and maximize our likelihood function,

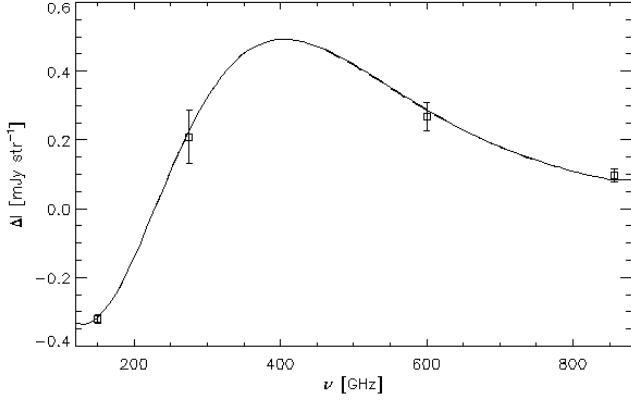


FIG. 2.— Sunyaev-Zel'dovich observations of the Bullet cluster (squares with error bars) as a function of frequency and best-fit models based on different electron velocity distributions (lines). The solid, dash-dotted, dashed, and dash-dot-dot-dotted lines are the best-fit models assuming relativistic (Jüttner), modified Jüttner with $\eta = 1$ and $\eta = 2$, and non-relativistic (Maxwellian) velocity distributions. Note that SZ models based on all of these distributions provide a good fit, thus the fitted models (lines) are indistinguishable.

$\mathcal{L} \sim \exp(-\chi^2)$ to determine the best-fit temperatures using different SZ effect models derived based on the Wright formalism (Section 4) assuming relativistic Jüttner (Equation 20), modified Jüttner with $\eta = 1$ and 2 (Equation 21), and non-relativistic, Maxwellian (Equation 19), velocity distribution functions. We do not consider models derived from the Kompaneets equation because it does not provide a good approximation for the nonrelativistic SZ effect at high frequencies (see Figure 1).

We show our results in Figure 2. The solid, dashed, dash-dotted, and dash-dot-dot-dotted, lines are the best-fit models assuming relativistic (Jüttner), modified Jüttner distributions with $\eta = 1$ and 2 , and non-relativistic (Maxwellian) EV distributions. The SZ model based on each one of these distributions provides a good fit, there is no significant difference in their χ^2 values ($\Delta\chi^2 < 1$). thus the fitted models (lines) are indistinguishable. We obtain good fits for all four models with best-fit electron temperatures of $T_J = 22.1^{+5.65}_{-4.97}$ keV, $T_{MJ1} = 23.0^{+6.16}_{-5.32}$ keV, $T_{MJ2} = 23.9^{+6.34}_{-5.57}$ keV, and $T_{MX} = 18.3^{+4.33}_{-3.76}$ keV, assuming Jüttner, modified Jüttner with $\eta = 1$ and $\eta = 2$, and Maxwellian EV distributions. Our result for the best-fit temperature, $T_J = 22$ keV, assuming the Jüttner EV distribution agrees with that obtained by Colafrancesco et al. (2011) assuming a single temperature gas and adopting the same velocity distribution function.

6. FITTING DIFFERENT VELOCITY DISTRIBUTION FUNCTIONS TO SIMULATED SZ OBSERVATIONS

We address the question: What accuracy do we need in the SZ observations to be able to derive more accurate temperatures and thus distinguish EV distribution functions with high significance? We proceed in two steps: First, we carry out Monte Carlo simulations to generate mock SZ observations assuming a fiducial EV distribution based on the Jüttner distribution function assuming a few per cent errors in the SZ measurements. Then we determine the best-fit temperatures (applying χ^2 statistic as in Section 5) using data from the same Monte Carlo realization of the SZ observations assuming different EV distribution functions, and compare the probability distributions of the temperatures. We are adopting modified Jüttner distributions only with $\eta = 1$ and 2 , since these are suggested by different approaches of relativistic kinetic the-

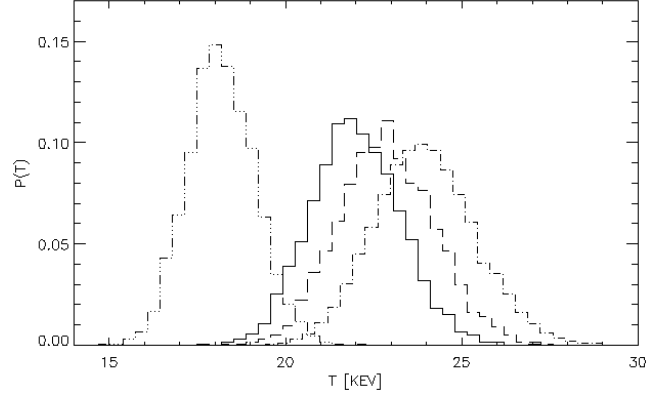


FIG. 3.— Probability distributions of best-fit temperatures from fitting SZ models based on the Jüttner, modified Jüttner with $\eta = 1$ and 2 , and Maxwellian electron velocity distributions to the same simulated SZ observations (solid, dashed, and dash-dotted, and dash-dot-dot-dotted lines). We assumed a Jüttner velocity distribution as our fiducial model with a temperature of 22.1 keV, and 5% errors in the SZ measurements.

ory (as described in Section 2). We found no theory resulting modified Jüttner distributions with $\eta > 2$. The distributions of the best-fit values can be used to determine the errors in the derived gas temperatures for the assumed per cent errors in the SZ amplitude measurement. Essentially, we use Monte Carlo simulations to propagate the errors from the SZ amplitude measurements to the derived temperatures.

6.1. Fitting to SZ observations of a single-temperature gas

In this section we assume a single temperature gas. For definiteness, motivated by our fit to the Bullet cluster data (Section 5), we adopt an electron temperature of 22.1 keV.

We display our results in Figure 3 assuming 5% error in the SZ measurements. In this figure we show probability distributions of the best-fit temperatures from fitting SZ models based on the Jüttner, $P_J(T)$, modified Jüttner with $\eta = 1$ and $\eta = 2$, $P_{MJ1}(T)$ and $P_{MJ2}(T)$, and Maxwellian, $P_{MX}(T)$, EV distributions to the same simulated SZ observations with solid, dashed, dash-dotted, and dash-dot-dot-dotted lines. As before, we find that each SZ model provides a good fit to the simulated data, and there is no significant difference between the fitted χ^2 values. The shapes of the fitted functions are very similar, they differ less than a fraction of 1% (the best-fit SZ models not shown, they would be indistinguishable, as in Figure 2). This agrees with the result of Prokhorov et al. (2011), who demonstrated that their method needs an accuracy of 0.1% in the SZ measurements to be able to distinguish between Maxwellian and Jüttner EV distributions.

Even though the best-fit SZ models based on different EV distributions are indistinguishable, we find, that the fitted temperatures are different: we obtained best-fit electron temperatures of $T_J = 22.1^{+1.25}_{-1.25}$ keV, $T_{MJ1} = 23.0^{+1.41}_{-1.41}$ keV, and $T_{MJ2} = 23.9^{+1.43}_{-1.43}$ keV, and $T_{MX} = 18.3^{+0.96}_{-0.96}$ keV for EV distributions of the form of Jüttner, modified Jüttner with $\eta = 1$ and 2 , and Maxwellian. The probability distributions for the best-fit temperatures assuming Maxwellian EV distribution ($P_{MX}[T]$) is well separated from those based on its three relativistic generalizations, the Jüttner and modified Jüttner velocity distributions with $\eta = 1$ and 2 ($P_J[T]$, $P_{MJ1}[T]$, and $P_{MJ2}[T]$; Figure 3), suggesting that the Maxwellian EV distribution function can be distinguished from the other three distributions. However, our results indicate that the Jüttner and modified Jüttner EV distribution functions cannot be distinguished based on their

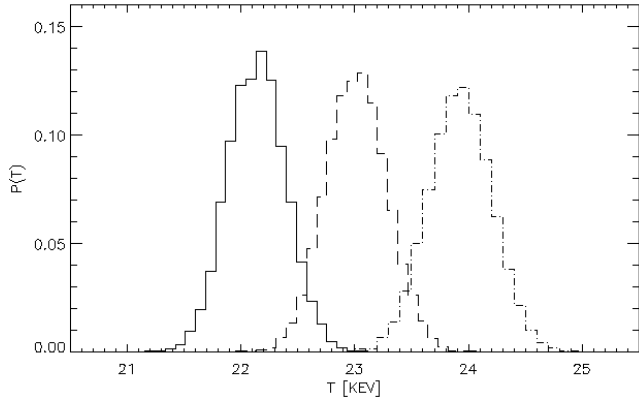


FIG. 4.— Same as Figure 3, assuming the same fiducial model and fitting SZ models based on the Jüttner and modified Jüttner electron velocity distributions with $\eta = 1$ and 2 (solid, dashed, and dash-dotted lines), but adopting measurement errors of 1% in the SZ effect.

temperatures assuming 5% accuracy in the SZ measurements.

We carried out Monte Carlo simulations to estimate the accuracy necessary to distinguish between the different relativistic velocity distributions: the Jüttner and modified Jüttner distributions. We used the same fiducial model as before: Jüttner EV distribution function with a temperature of 22.1 keV, but this time we assumed 1% measurement error in the SZ observations. The probability distributions of best-fit temperatures from fitting SZ models based on the Jüttner, $P_J(T)$, and modified Jüttner electron velocity distributions with $\eta = 1$ and 2, $P_{MJ1}(T)$ and $P_{MJ2}(T)$ to the same simulated SZ observations (solid, dashed, and dash-dotted lines) are shown in Figure 4.

Again, we find that all models provide a good fit to the simulated data, the shape of the fitted SZ models are very similar. However, the fitted temperatures are different: we obtain a good fit for all three models with best-fit electron temperatures: $T_J = 22.1^{+0.25}_{-0.25}$ keV, $T_{MJ1} = 23.0^{+0.27}_{-0.27}$ keV, $T_{MJ2} = 23.9^{+0.28}_{-0.28}$ keV assuming Jüttner and modified Jüttner EV distributions with $\eta = 1$ and 2. Note that the best-fit temperatures are the same for these two EV distribution functions as before, since we used the same fiducial models. The differences are only in the errors in the derived temperatures, which are much smaller as a consequence of our adopted smaller errors in the SZ amplitudes. The probability distributions for the best-fit temperatures assuming Jüttner ($P_J[T]$) and modified Jüttner ($P_{MJ1}[T]$, $P_{MJ2}[T]$) velocity distributions are well-separated (Figure 4), suggesting that a 1% error in the SZ measurements would allow us to distinguish between them.

6.2. Fitting to SZ observations of a shock from a merging cluster simulation

In the previous section we demonstrated that, in the case of a single temperature gas, SZ measurements with an accuracy of 1% at four frequencies may be used to distinguish between EV distribution functions of the form of non-relativistic Maxwellian, Jüttner, and modified Jüttner. However, any LOS through a galaxy cluster contains a range of temperatures, even if the cluster is in dynamical equilibrium. It is also difficult to model clusters because they are not spherical, may be dynamically active, and contain substructure.

In this section we use our N -body/hydrodynamical simulation of a merging galaxy cluster to test our method to distinguish between EV distribution functions. Our simulation was carried out using FLASH, an Eulerian N -body/hydrodynamical code developed at the Center for Astrophysical Thermonu-

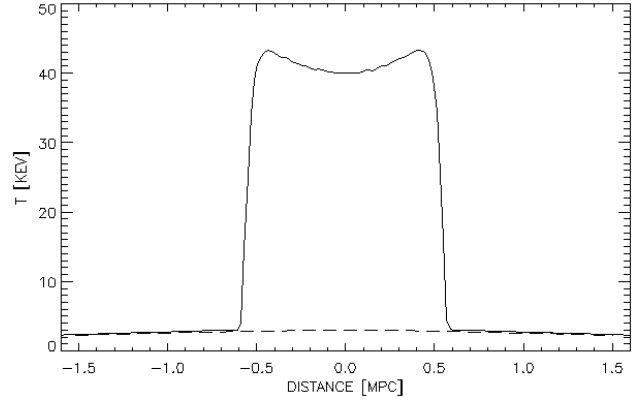


FIG. 5.— Temperature distribution along the LOS through a shock and a pre-shocked region near the shock extracted from a merging cluster N -body/hydrodynamical simulation (solid and dashed lines; see text for details).

clear Flashes at the University of Chicago (Fryxell et al. 2000; Ricker 2008). We used our well-tested method to setup and run the simulation (e.g., Molnar & Broadhurst 2015, 2017, 2018). For a detailed description of our method, see Molnar et al. (2012). We adopted initial total masses of $1.7 \times 10^{15} M_\odot$ and $1.6 \times 10^{15} M_\odot$ (main and infalling cluster), an impact parameter of 100 kpc, and an infall velocity of 2500 km s^{-1} in our simulation.

We chose an epoch soon after the 1st core passage from our outputs, when a bow shock is moving ahead of the infalling cluster. The Mach number for this shock is 6.51, and the shock velocity is 5740 km s^{-1} . We extract data using a viewing angle assuming that the two cluster centers and their relative velocities are in the plane of the sky. We choose a LOS close to the edge of the bow shock. We show the temperature distribution along this LOS in Figure 5 (solid line). The temperature along a LOS through the pre-shocked gas near the shock is shown with a dashed line. The average temperature through the LOS of the pre-shocked gas is 2.68 keV with a 8.5% dispersion, while the average temperature of the pre-shock region in the LOS through the shocked gas (low temperature region of the LOS through the shocked gas in Figure 5) is 2.64 keV with a 8.8% dispersion. The average temperature in the shocked region is 42.1 keV with a 2% dispersion. Thus, we can identify two phases of the gas in the LOS through the shock: one lower and one with temperature phase corresponding to the pre-shocked and shocked regions, with a less than 9% dispersion, much less than the difference between the average temperatures (42.1 keV vs. 2.68 keV). These results suggest that we may adopt a two temperature model for the gas in the LOS through the shock.

We expected that fitting two temperature models to SZ data points at only four frequencies would not constrain the EV distribution functions well, thus we assumed measurements at the *Planck/Herschel* frequencies ($\nu = 30, 44, 70, 100, 143, 217, 353, 545, 600, \text{ and } 857 \text{ GHz}$). Carrying out Monte Carlo simulations assuming 1% error in the SZ amplitudes, we found that the distributions of the best-fit temperatures were not well separated, thus these set of frequencies do not make it possible to distinguish between Jüttner and modified Jüttner EV distributions. We repeated our simulations adding more measurements around the steep slope at frequencies between 217 and 353 GHz (244.4, 272.8, 06.9 GHz), but that did not improve much the accuracy in the best-fit temperatures. We found that adding 1080 GHz, to the *Planck/Herschel* fre-

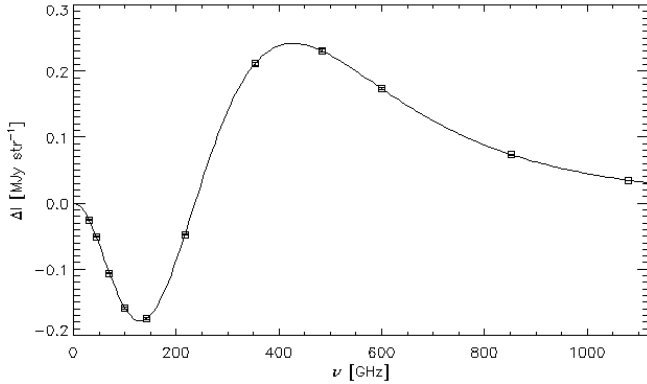


FIG. 6.— Mock SZ observations along a LOS through a shock extracted from a merging cluster N -body/hydrodynamical simulation assuming 1% error in the SZ amplitudes (squares with error bars). The temperature distribution in this LOS is shown with a solid line in Figure 5. We adopted a Jüttner electron velocity distribution to generate the SZ signal (solid line; see text for details).

quencies to capture the fall off of the SZ signal at very high frequencies improved on the accuracy in the best-fit temperatures significantly. The SZ signal from a low temperature gas (a few keV) at very high frequencies (above ~ 900 GHz) is negligible, but provide strong constraints on high temperature gas. We show the simulated SZ observations at these extended *Planck/Herschel* frequencies and the underlying SZ model through a LOS containing a shock in Figure 6 (squares with error bars and solid line).

We fitted a two temperature model to the mock SZ observations of the LOS through the shocked region, but found that the temperature of the pre-shocked gas was not constrained well. However, since the temperature of the pre-shocked gas in the LOS through the shock is very close to that in the LOS through the pre-shocked gas (see Figure 5), we fixed the temperature of the pre-shocked gas we derived using the LOS through a nearby pre-shocked region. The best fit value in a LOS through the pre-shocked region was 2.78 keV with a $\pm 3\%$ error, which is a very good match with the average value derived directly from our FLASH simulations (2.68 keV). It is also very close to the temperature of the pre-shocked gas in the LOS through the shock derived from our hydrodynamical simulation (2.65 keV). Therefore we fixed the lower temperature component at 2.78 keV, and fit SZ models based on the Jüttner and modified Jüttner EV distributions to the temperature of the shocked gas. We show the distributions of the best-fit temperatures assuming Jüttner and modified Jüttner EV distributions with $\eta = 1$ and $\eta = 2$ in Figure 7 (solid, dashed, and dash-dotted histograms).

Again, we obtain good fits for both models with different best-fit electron temperatures for the shocked region, $T_J = 42.1 \pm 0.88$ keV, $T_{MJ1} = 45.0 \pm 0.99$ keV, and $T_{MJ2} = 48.2 \pm 1.12$ keV, assuming Jüttner and modified Jüttner EV distributions with $\eta = 1$ and 2. The best-fit shock temperature, $T_J = 42.1$ keV is a very good match with the average temperature we obtained directly from our FLASH simulation (42.1 keV). As we can see from Figure 7, the probability distributions for the best-fit temperatures assuming Jüttner ($P_J[T]$) and modified Jüttner $P_{MJ1}[T]$, $P_{MJ2}[T]$ velocity distributions are clearly separated, suggesting that a 1% error in the SZ measurements would allow us to distinguish between these distribution functions.

7. DISCUSSION

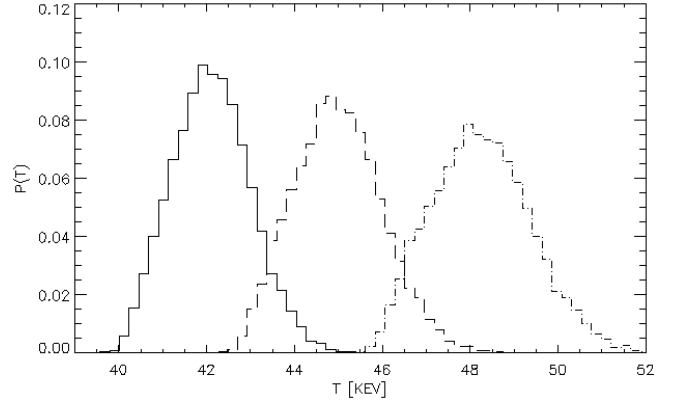


FIG. 7.— Probability distributions of best-fit shock temperatures from fitting SZ models based on the Jüttner and modified Jüttner electron velocity distributions with $\eta = 1$ and 2 (solid, dashed, and dash-dotted lines) to mock observations of a LOS through a shock extracted from a merging cluster N -body/hydrodynamical simulation (shown in Figure 6).

The low density, high temperature ICG in clusters of galaxies provides a unique laboratory to test the proposed EV distribution functions. The temperature in the ICG is not high enough for particle pair creation and annihilation to be important, thus we expect that an equilibrium particle velocity distribution function based on particle number conservation can be found. Also, the assumption of local thermodynamical equilibrium (LTE), which is a fundamental criterion for the existence of an equilibrium particle velocity distribution, should be valid in the ICG in relaxed galaxy clusters. The LTE should also be valid in merging clusters, because the time scale for the EV distribution to reach equilibrium is shorter than the time scale for galaxy cluster merging (e.g., Prokhorov et al. 2011).

Prokhorov et al. (2011) investigated the possibility to constrain the EV distribution in the ICG based on multi-frequency SZ observations. They assumed a temperature of 15.3 keV for the ICG, appropriate for a high-mass galaxy cluster and considered Maxwellian and its relativistic generalization, the Jüttner EV distribution functions. Prokhorov et al. expanded the velocity distribution functions in Fourier series and used the Wright formalism for the relativistic (Jüttner) distribution to derive equations for the Fourier coefficients. Comparing the coefficients, they concluded that the Maxwellian and Jüttner velocity distributions can be distinguished if the SZ amplitude is measured with 0.1% accuracy. They verified their conclusion with Monte Carlo simulations. Prokhorov et al. also pointed out the importance of high-frequency SZ observations (e.g. 375–860 GHz) in constraining EV distribution functions based on the SZ effect.

The Bullet cluster is one of the high-infall velocity merging galaxy clusters, which provided the first direct evidence for the existence of dark matter based on gravitational lensing (Clowe et al. 2006). The offsets between the mass surface density centers derived from lensing and the corresponding X-ray emission peaks marking centers of the gas (baryonic) components were significant (200–300 kpc, e.g., Paraficz et al. 2016). Multi-frequency radio/submm observations of the Bullet cluster are available at four frequencies from 150 GHz to 857 GHz, which makes it an excellent target for SZ studies (see Section 5).

Colafrancesco et al. (2011) fitted models to SZ observations of the Bullet cluster assuming a single and a double temperature thermal models for the ICG, and a sum of a single tem-

perature model and one with a non-thermal EV distribution. They assumed a Jüttner EV distribution for their thermal models. Colafrancesco et al. found that a thermal model with a temperature of $T = 22$ keV and optical depth $\tau = 8.3 \times 10^{-3}$, and a model consisting a sum of one thermal and one non-thermal EV models provide the best fits (no significant difference in the reduced χ^2). They fixed the temperature of the later model at the value derived from X-ray measurements ($T_X = 13.9 \pm 0.7$ keV; Govoni et al. 2004). Colafrancesco et al. argued that their later model with a sum of thermal and non-thermal plasma is more plausible because: 1) observations suggest the existence of a non-thermal electron component in the Bullet cluster (Ajello et al. 2010; Petrosian et al. 2006), and 2) their single component thermal model has a best-fit temperature of $T = 22$ keV, which is much higher than the one derived from X-ray observations assuming a single temperature model ($T_X = 13.9$ keV).

Chandra observations of the Bullet cluster found that the projected temperature in the Bullet cluster ranges between 4 and 30 keV, but the projected temperature in the LOS of the SZ center is about 15 keV (Govoni et al. 2004; Markevitch 2006). We expect that in the LOS going through the SZ centroid the ICG has a wide range of temperatures. In merging clusters, the physical gas temperature can be substantially reduced due to projection effects, as it was demonstrated quantitatively using hydrodynamical simulations (see Figure 4 in Molnar & Broadhurst 2017).

In order to demonstrate our new method, we fitted single temperature EV models to SZ observations of the Bullet cluster, and obtained best-fit temperatures of $T_{MX} = 18$ keV, $T_J = 22$ keV, $T_{MJ1} = 23$ keV, and $T_{MJ2} = 24$ keV assuming Maxwellian, Jüttner, modified Jüttner EV distributions with $\eta = 1$ and 2 (see Section 5). The best-fit temperature, $T_J = 22$ keV, of our single-temperature model assuming the Jüttner EV distribution (Section 5) agrees with that obtained by Colafrancesco et al. (2011) assuming a single temperature gas adopting the same velocity distribution function. All three models provided a good fit with no significant difference in their χ^2 values ($\Delta\chi^2 < 1$).

Even though the differences in the fitted temperatures between SZ models based on the Maxwellian EV distribution and those using Jüttner and modified Jüttner distributions are as large as $T_J - T_{MX} = 4$ keV, $T_{MJ1} - T_{MX} = 5$ keV, and $T_{MJ2} - T_{MX} = 6$ keV, the error bars on these temperatures are even larger ($\sim 5 - 6$ keV), thus we cannot distinguish between these EV models based on the best-fit temperatures.

The projected temperature from X-ray observations of the Bullet cluster through the SZ centroid is 15 keV, which would be consistent with the temperature we derived from the SZ observations assuming Maxwellian EV distribution (and more than 1σ smaller than the temperatures derived assuming its relativistic generalizations), but this X-ray temperature is not reliable due to projection effects (e.g., Molnar & Broadhurst 2017). The SZ signal was derived from these observations along a LOS through the center of the Bullet cluster, which may be contaminated by a high energy, nonthermal electron population. Dedicated SZ observations through a LOS which has no contamination by nonthermal electrons might simplify the modeling of the cluster SZ signal. However, the bullet cluster is a large-infall velocity merging cluster, thus its LOS temperature structure can only be determined by dedicated N -body/hydrodynamical simulations. The numerical simulations could provide a more realistic model for the LOS distri-

bution of the density and temperature in the ICG to derive the SZ effect amplitude as a function of frequency.

We obtained similar results fitting the same EV distribution models to mock SZ observations adopting a fiducial model based on the Jüttner distribution with electron temperature of 22 keV (motivated by our results from fitting models to SZ observations of the Bullet cluster) assuming a few percent error in the observations (Section 6.1). The best fit temperatures assuming Jüttner, modified Jüttner, and Maxwellian EV distributions were $T_J = 22$ keV, $T_{MJ1} = 23$ keV, $T_{MJ2} = 24$ keV, and $T_{MX} = 18$ keV, in agreement with our fits to the Bullet cluster data, but the error bars for the temperatures were smaller. We noticed, that the best-fit temperatures may differ as much as 1 – 6 keV depending on which model we assume for the velocity distribution. These results suggest that, if we can derive the ICG temperature from a different, independent method, we may be able to distinguish between the proposed EV distributions. Based on our results, we propose a new method to constrain the electron velocity distribution in the ICG making use of the frequency distribution of the SZ effect. Our method consists of two steps: 1) derive the temperature from fitting models to SZ observations based on different EV distribution functions; 2) compare the derived temperatures to a temperature obtained using an independent (e.g., X-ray) method.

Such independent method may be provided by high-spectral and spectral resolution X-ray observations, which could measure accurate temperatures in the ICG based on emission lines. This method would have less projection bias than the conventional one using low spectral-resolution wide spectra. In principle, measuring thermal line broadening would allow us to derive gas temperatures in clusters, but it may be difficult to separate it from broadening due to turbulence or resonant line scattering (e.g., Inogamov & Sunyaev 2003; Molnar 2016). Line ratios may provide a better diagnostic of gas temperatures in clusters (e.g., Nevalainen et al. 2003). Note, however, that models for X-ray emission lines should be calculated consistently, using the appropriate EV distribution functions (e.g., using the method developed by Prokhorov et al. 2009).

We carried out Monte Carlo simulations of SZ measurements of a single-temperature gas to estimate the accuracy needed to distinguish between different EV distribution functions. Fitting to mock SZ observations assuming a 5% error in the SZ measurements we found that the relativistic generalizations of the Maxwell velocity distribution, cannot be distinguished from each other, but they can be distinguished from the Maxwellian velocity distribution, since the probability distribution of best-fitted temperatures assuming Maxwellian velocity distribution, $P_{MX}(T)$, is clearly separated from those based on the Jüttner and modified Jüttner distributions with $\eta = 1$ and 2, $P_J(T)$, $P_{MJ1}(T)$, and $P_{MJ2}(T)$ (see Figure 3). Assuming that the temperature can be derived using another method with the same accuracy as the one based on the SZ observations assuming 5% errors in the SZ amplitudes (~ 1.25 keV), we can still distinguish between the Maxwellian and its relativistic generalizations, the Jüttner, and the modified Jüttner distributions with high significance ($\sim 2\sigma$). In order to distinguish between different relativistic generalizations of the Maxwell velocity distribution we need more accurate SZ measurements than 5%. The significance of measuring SZ effect with 5% accuracy is that it could justify the usage of relativistic generalizations of the Maxwell velocity distributions in studying the ICG in galaxy clusters.

As we discussed it in Section 2, there are difficulties in de-

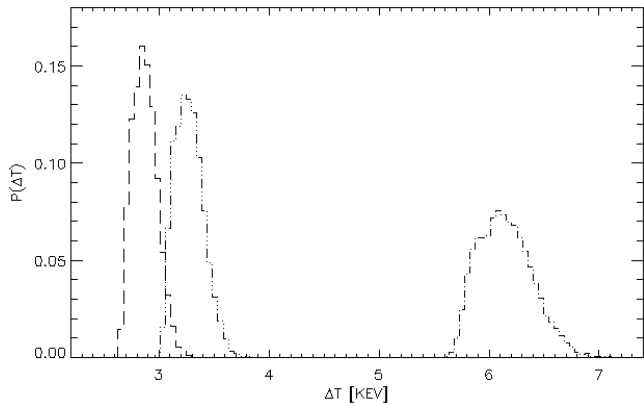


FIG. 8.— Probability distributions of the differences of the best-fit shock temperatures from fitting SZ models to mock observations of a line of sight through a shock extracted from a merging cluster simulation assuming 1% errors in measurements. Dashed and dash-dotted lines show differences between best-fit temperatures based on the Jüttner and modified Jüttner electron velocity distributions with $\eta = 1$ ($T_{MJ1} - T_J$) and $\eta = 2$ ($T_{MJ2} - T_J$). The dash-dot-dot-dotted line represents temperature differences between assuming modified Jüttner distributions with $\eta = 1$ and $\eta = 2$ ($T_{MJ2} - T_{MJ1}$).

veloping a self-consistent extension of our nonrelativistic kinetic theory to the relativistic regime. Therefore, it would be of fundamental importance to use the SZ effect to verify which relativistic generalization of the Maxwell distribution is correct: the Jüttner or one of the modified Jüttner distributions. This would provide us an empirical test for different relativistic generalizations of our non-relativistic kinetic theory. Fitting to mock SZ observations as before, but assuming 1% errors in the SZ measurements we find that the probability distributions of best-fit temperatures from fitting SZ models based on the Jüttner, $P_J(T)$, and modified Jüttner EV distributions with $\eta = 1$ and $\eta = 2$, $P_{MJ1}(T)$, and $P_{MJ2}(T)$, to the same simulated SZ observations are well separated (Figure 4), thus we can distinguish them. Assuming that the measurement error in the temperature of the ICG in a cluster is ± 0.9 keV (3σ) based on another method, our results suggest that we can distinguish between the Jüttner and modified Jüttner EV distributions with $\eta = 1$ with high significance ($\sim 3\sigma$). Measuring the gas temperature with an error of ± 1.8 keV (3σ) with another method, we expect that we can distinguish between the Jüttner and modified Jüttner distribution with $\eta = 2$ with high significance ($\sim 3\sigma$). In order to distinguish between modified Jüttner distributions with $\eta = 1$ and $\eta = 2$, we would need an accuracy of about ± 1.0 keV. Note, that 1% errors in the SZ measurements are already achievable with some instruments (e.g., *Herschel*-SPIRE; Griffin et al. 2010).

We demonstrated that our method can be used to distinguish between different EV distribution functions if the gas has a single temperature. However, any LOS through a galaxy cluster has a range of temperatures, even if the cluster is relaxed. In order to test our proposed method to EV distribution functions in a more realistic cluster model, we fitted to mock SZ observations as before to a LOS through a shock extracted from our self-consistent N -body/hydrodynamical simulation assuming 1% errors in the SZ measurements at the *Planck*/*Herschel* frequencies and an additional high frequency (1080 GHz). Again, we found that the probability distributions of best-fit temperatures from fitting SZ models based on the Jüttner, $P_J(T)$, and modified Jüttner EV distributions with $\eta = 1$ and 2, $P_{MJ1}(T)$ and $P_{MJ2}(T)$, to simulated SZ observations are well separated (Figure 7), thus we can distinguish them. We show the probability distribution of the differences in the best-

fit temperatures in a LOS through a shock using EV distributions of the form of Jüttner and modified Jüttner with $\eta = 1$ and 2 in Figure 8. In this Figure, dashed and dash-dotted lines show the distribution of best-fit temperature differences between assuming Jüttner and modified Jüttner EV distributions with $\eta = 1$ ($T_{MJ1} - T_J$) and $\eta = 2$ ($T_{MJ2} - T_J$). Best-fit temperature differences between based on modified Jüttner distributions with $\eta = 1$ and $\eta = 2$ ($T_{MJ2} - T_{MJ1}$) are displayed with a dash-dot-dot-dotted line. We find that assuming that the 3σ measurement error in the temperature of the ICG in a cluster is ± 2.65 keV (± 5.65 keV) based on another method, our results suggest that we can distinguish between the Jüttner and the modified Jüttner EV distributions with $\eta = 1$ ($\eta = 2$) with high significance ($\sim 3\sigma$). In order to distinguish between modified Jüttner distributions with $\eta = 1$ and $\eta = 2$ with high significance ($\sim 3\sigma$), we would need to measure the ICG temperature with an error of ± 2.98 keV (3σ) using another method, similar to the requirement for distinguishing between Jüttner and modified Jüttner distribution with $\eta = 1$.

In general, higher temperature ICG would make it easier the test EV distribution functions. We found that, for gas temperatures of ~ 20 keV and ~ 40 keV, the differences between the best-fit temperatures assuming Jüttner and a modified Jüttner EV distribution with $\eta = 1$, $T_{MJ1} - T_J$, are 4% and 7%, while for temperatures adopting a modified Jüttner distribution with $\eta = 2$, the differences, $T_{MJ2} - T_J$, are 8% and 14%. Based on our results, we expect that for shock temperatures of ~ 60 keV, the differences between best-fit temperatures for $T_{MJ1} - T_J$, $T_{MJ2} - T_J$, and $T_{MJ2} - T_{MJ1}$ would be about 14%, 21%, and 15%, much easier the achieve.

The observational frequencies could be chosen to minimize the errors in the temperature derivations based on different EV distribution models. High-spectral and spatial resolution radio/submm observations may help to separate some of the contaminating components by choosing LOSs avoiding substructures and radio halos and relics containing high energy nonthermal electrons. Radio relics associated with shocks are patchy in most merging clusters, thus they can be avoided (e.g., except the ‘‘Sausage cluster’’, although it can be modeled with N -body/hydrodynamical simulations; Molnar & Broadhurst 2017). Also, it will be necessary to identify other methods to derive accurate temperatures in the ICG. X-ray emission lines from the ICG may provide the required accuracy. A dedicated feasibility study would be important based on more realistic ICG cluster models taking into account the response of the available detectors (spectral and spatial resolution, sensitivity, etc.), and contaminating effects in conjunction with an analysis of other, independent, methods to derive the temperature in the ICG. We leave this detailed analysis for the future.

8. CONCLUSION

We developed a new method to test relativistic kinetic theories based on observations of the thermal SZ effect in galaxy clusters. We demonstrated that the frequency dependence of the SZ effect can be used to distinguish different EV equilibrium distribution functions in the ICG assuming that an independent measurement of the temperature is available from another method. This new method is based on our observation that different EV distribution functions result in different temperatures when their models are fitted to the same SZ data.

We found that a 5% accuracy is necessary in the SZ amplitude measurements of high single temperature gas (~ 20 keV)

to distinguish between non-relativistic (Maxwellian), and its relativistic generalizations, the Jüttner and the modified Jüttner EV distributions. In order to identify the correct relativistic generalization of the Maxwell velocity distribution as the Jüttner or one of the modified Jüttner EV distributions, we would need about 1% errors in the measured SZ amplitudes.

We demonstrated that our method works in a simulated merging cluster using a LOS through a shocked region. A LOS through a shock contains two phases of the gas: shocked and pre-shocked gas, with a range of temperatures. We found that the change of the temperature within each phase is relatively small. We carried out Monte Carlo simulations assuming a 1% error in the SZ measurements at the *Planck/Herschel* frequencies and at 1080 GHz. We found that two temperature gas models based on Jüttner and modified Jüttner EV distributions with $\eta = 1$ and 2 fit well to the mock SZ observations. Our results suggest that these three distributions can be distinguished with high significance based on their best-fit temperatures to the high temperature $\gtrsim 40$ keV shocked gas in clusters of galaxies. We found that in order to reach high significance in distinguishing between Jüttner and modified Jüttner EV distributions we need observations at THz frequencies. Astrophysics in the THz frequency range is a promising new field covering a wide range of research topics

from black holes to exoplanets and cosmology (e.g., [Gurvits et al. 2019](#); [Withington 2004](#)). There are atmospheric windows at e.g., ~ 1.1 THz, and ~ 1.5 THz, which make ground-based observations available at high altitude, dry observing sites (e.g., from Antarctica ([Seta et al. 2013](#))). Using heterodyne arrays on board of SOFIA balloon experiment, observations have already been made between 1.8 THz and 4.7 THz ([Risacher et al. 2018](#)), and more ground and space based THz telescopes are under development (e.g., [Gurvits et al. 2019](#)).

Our results suggest that it would be worth while to carry out a feasibility study of our proposed new method to constrain EV distributions in the ICG based on more realistic cluster models derived from hydrodynamical cosmological simulations. Systematic effects from inhomogeneous temperature distribution, substructures and nonthermal electron populations could be studied using clusters from cosmological simulations.

We thank the referee for detailed comments and suggestions, which helped to improve our paper. This work was supported in part by the Ministry of Science and Technology of Taiwan (grants MOST 106-2628-M-001-003-MY3 and MOST 109-2112-M-001-018-MY3) and by Academia Sinica (grant ASIA-107-M01).

REFERENCES

- Ajello, M., Rebusco, P., Cappelluti, N., et al. 2010, *ApJ*, 725, 1688
 Aragon-Munoz, L. & G. Chacon-Acosta, G. 2018, *J. Phys.: Conf. Ser.* 1030 012004
 Baldi, A. S., Bourdin, H., Mazzotta, P., et al. 2019, *A&A*, 630, A121
 Bernstein, J. 2004, *Kinetic Theory in the Expanding Universe*, Cambridge University Press, Cambridge
 Birkinshaw, M. 1999, *Phys. Rep.*, 310, 97
 Bourdin, H., Mazzotta, P., Kozmany, A., et al. 2017, *ApJ*, 843, 72
 Carlstrom, J. E., Holder, G. P., & Reese, E. D., 2002, *ARA&A*, 40, 643
 Chandrasekhar, S. 1960, New York: Dover, 1960
 Clowe, D., Bradač, M., Gonzalez, A. H., et al. 2006, *ApJ*, 648, L109
 Colafrancesco, S., & Marchegiani, P. 2010, *A&A*, 520, A31
 Colafrancesco, S., Marchegiani, P., & Buonanno, R. 2011, *A&A*, 527, L1
 Colafrancesco, S., Prokhorov, D., & Dogiel, V. 2009, *A&A*, 494, 1
 Cubero, D., Casado-Pascual, J., Dunkel, J., et al. 2007, *Phys. Rev. Lett.*, 99, 170601
 Dunkel, J., & Hänggi, P. 2007, *Physica A Statistical Mechanics and its Applications*, 374, 559
 Dunkel, J., Hänggi, P., & Hilbert, S. 2009, *Nature Physics*, 5, 741
 Dunkel, J., Talkner, P., & Hänggi, P. 2007, *New Journal of Physics*, 9, 144
 Fryxell, B., et al. 2000, *ApJS*, 131, 273
 Gomez, P., Romer, A. K., Peterson, J. B., et al. 2004, *Plasmas in the Laboratory and in the Universe: New Insights and New Challenges*, 361
 Govoni, F., Markevitch, M., Vikhlinin, A., et al. 2004, *ApJ*, 605, 695
 Gurvits, L. I., Paragi, Z., Casasola, V., et al. 2019, arXiv e-prints, arXiv:1908.10767
 R, Hakim, 2011, "Introduction to relativistic statistical mechanics : classical and quantum", World scientific, Singapore
 Halverson, N. W., Lanting, T., Ade, P. A. R., et al. 2009, *ApJ*, 701, 42
 Hansen, S. H., Pastor, S., & Semikoz, D. V. 2002, *ApJ*, 573, L69
 Horwitz, L. P., & Piron, C. 1973, *Helv. Phys. Acta*, 46, 316
 Horwitz, L. P., Shashoua, S., & Schieve, W. C. 1989, *Physica A Statistical Mechanics and its Applications*, 161, 300
 Horwitz, L. P., Schieve, W. C., & Piron, C. 1981, *Annals of Physics*, 137, 306
 Griffin, M. J., Abergel, A., Abreu, A., et al. 2010, *A&A*, 518, L3
 Inogamov, N. A., & Sunyaev, R. A. 2003, *Astronomy Letters*, 29, 791
 Jüttner, F. 1911, *Annalen der Physik*, 339, 856
 Kaniadakis, G. 2006, *Physica A Statistical Mechanics and its Applications*, 365, 17 [197] G. Kaniadakis. Towards a relativistic statistical theory. *Physica A*, 365:17–23, 2006
 Kompaneets, A. S. 1957, *Soviet Journal of Experimental and Theoretical Physics*, 4, 730
 Lehmann, E. 2006, *Journal of Mathematical Physics*, 47, 023303
 Leutwyler, H. 1965, *Il Nuovo Cimento*, 37, 556
 Markevitch, M. 2006, *The X-ray Universe 2005*, 723
 Marmo, G., Mukunda, N., & Sudarshan, E. C. G. 1984, *Phys. Rev. D*, 30, 2110
 Molnar, S. M., Hearn, N. C., & Stadel, J. G. 2012, *ApJ*, 748, 45
 Molnar, S. M., 2015, *Cosmology with Clusters of Galaxies*, Nova Science Publishers, New York
 Molnar, S. 2016, *Front. Astron. Space Sci.*, 2, 7
 Molnar, S. M., & Birkinshaw, M. 1999, *ApJ*, 523, 78
 Molnar, S. M., & Broadhurst, T. 2015, *ApJ*, 800, 37
 Molnar, S. M., & Broadhurst, T. 2017, *ApJ*, 841, 46
 Molnar, S. M., & Broadhurst, T. 2018, *ApJ*, 862, 112
 Montakhab, A., Ghodrati, M., & Barati, M. 2009, *Phys. Rev. E*, 79, 031124
 Nevalainen, J., Lieu, R., Bonamente, M., et al. 2003, *ApJ*, 584, 716
 Nozawa, S., Itoh, N., & Kohyama, Y. 1998, *ApJ*, 507, 530
 Paraficz, D., Kneib, J.-P., Richard, J., et al. 2016, *A&A*, 594, A121
 Peano, F., Marti, M., Silva, L. O., et al. 2009, *Phys. Rev. E*, 79, 025701
 Petrosian, V., Madejski, G., & Luli, K. 2006, *ApJ*, 652, 948
 Plagge, T., Benson, B. A., Ade, P. A. R., et al. 2010, *ApJ*, 716, 1118
 Planck Collaboration, Aghanim, N., Arnaud, M., et al. 2016, *A&A*, 594, A22
 Pointecouteau, E., Giard, M., & Barret, D. 1998, *A&A*, 336, 44
 Prokhorov, D. A., Colafrancesco, S., Akahori, T., et al. 2011, *A&A*, 529, A39
 Prokhorov, D. A., Dubois, Y., & Nagataki, S. 2010, *A&A*, 524, A89
 Prokhorov, D. A., Durret, F., Dogiel, V., et al. 2009, *A&A*, 496, 25
 Rephaeli, Y. 1995, *ApJ*, 445, 33
 Ricker, P. M. 2008, *ApJS*, 176, 293
 Risacher, C., Güsten, R., Stutzki, J., et al. 2018, *Journal of Astronomical Instrumentation*, 7, 1840014
 Schieve, W. C. 2005, *Foundations of Physics*, 35, 1359
 Seta, M., Nakai, N., Shun Ishii, S., et al. 2013, in *Astrophysics from Antarctica, Proceedings IAU Symposium No. 288, 2012*, eds.: Burton, M., G., Cui, X., & Tothill, N. F. H.
 Sunyaev, R. A., & Zeldovich, I. B. 1980, *ARA&A*, 18, 537
 Sygne, J. L., 1957, *The Relativistic Gas*, North-Holland, Amsterdam
 van Hees, H., Greco, V., & Rapp, R. 2006, *Phys. Rev. C*, 73, 034913
 Withington, S. 2004, *Philosophical Transactions of the Royal Society of London Series A*, 362, 395
 Wright, E. L. 1979, *ApJ*, 232, 348
 Zemcov, M., Rex, M., Rawle, T. D., et al. 2010, *A&A*, 518, L16